

Net 212.5 Gbit/s Transmission in O-band With a SiP MZM, One Driver and Linear Equalization

Maxime Jacques^{1,*}, Zhenping Xing¹, Alireza Samani¹, Xueyang Li¹, Eslam El-Fiky¹, Samiul Alam¹, Olivier Carpentier¹, Ping-Chiek Koh², and David V. Plant¹

¹Department of Electrical and Computer Engineering, McGill University, Montréal, QC H3A 2A7, Canada

²Lumentum LLC, 1001 Ridder Park Dr, San Jose, CA 95131, USA

maxime.jacques@mail.mcgill.ca

Abstract: We present an O-band SiP MZM design enabling net transmission of 212.5 (200) Gbit/s over 2 (10) km using PAM-8 modulation and 20% SD-FEC, and net 200 Gbit/s back-to-back using PAM-6 and 6.7% HD-FEC. © 2020 The Author(s)

1. Introduction

The exponential growth in data center IP traffic entails rapidly evolving standards and corresponding optical transceiver solutions. Whereas current 100 GbE products are dominant today, the new 400 GbE generation of interconnects is starting to be deployed [1]. The future generation of highly parallel pluggable module standards could move to 8×100 Gbit/s PAM-4 (800 Gbit/s) or directly to 8×200 Gbit/s (1.6 Tb/s links), assuming a QSFP-DD form factor [2]. Technology-wise, transceivers based on silicon photonics (SiP) are now estimated to account for >25% of products for distances of 500 m and beyond [1], and their importance will keep growing as market volume increases due their cost effectiveness and high yield. Hence, for the data center space, the development of practical and low-power SiP transceivers operating in O-band at net rates >200 Gbit/s/ λ is an important target. Furthermore, solutions incorporating simple hard-decision forward error correction (HD-FEC) would be ideal for these applications.

SiP IQ modulators operating at 64 Gbaud 64-QAM [3] and 100 Gbaud 32-QAM [4] were recently reported, leveraging the high sensitivity of coherent receivers and complex digital signal processing (DSP). In intensity modulation direct-detection (IM/DD) links, 166.7 Gbit/s net rate transmission over 1 km was demonstrated using a dual-drive SiP travelling-wave Mach-Zehnder modulator (TW-MZM), non-linear post-equalization and maximum likelihood sequence detection (MLSD) to compensate for the poor modulator bandwidth [5]. Since MLSD implies latency and M^2 trellis path computations at each received symbol, where M is the modulation order, its adoption is unlikely in commercial low-cost transceivers. Recently, we reported for the first time transmission of net 200 Gbit/s on a single wavelength with a SiP modulator in an IM/DD system, using a segmented MZM, two drivers and soft-decision forward error correction (SD-FEC) [6]. However, at very high symbol rates, the picosecond precision required on the phase alignment of the two MZM segment drive signals would be challenging for practical RF delay lines.

In this paper, we present the design and characterization of a single-segment, single-driver O-band SiP MZM allowing for >200 Gbit/s/ λ net rate operation. Fabrication on a silicon-on-insulator (SOI) wafer was carried out in a commercial foundry. The MZM has a measured bandwidth/ V_π figure of merit (BW/ V_π FOM) of 8.7 GHz/V at -2 V bias. Using only linear feed-forward equalization (FFE), it enables 85 Gbaud PAM-8 (net 212.5 Gbit/s) transmission over 2 km and 80 Gbaud PAM-8 (net 200 Gbit/s) transmission over 10 km with SD-FEC, as well as 85.5 Gbaud PAM-6 (net 200 Gbit/s) back-to-back (B2B) transmission and 100 Gbaud PAM-4 (net 187 Gbit/s) 2 km transmission under the $3.8E-03$ hard-decision (HD) FEC threshold. To the best of our knowledge, this is the fastest net rate and first 200 Gbit/s net rate using HD-FEC reported for a SiP MZM in a direct-detection system. It is also the first such demonstration using a single-drive SiP MZM. At 80 Gbaud PAM-8 (net 200 Gbit/s) B2B, the MZM drive voltage can be reduced to 2.1 Vpp at the SD-FEC threshold, which translates to a dynamic modulator energy consumption of only 51 fJ/bit.

2. Design, Fabrication and Characterization

The MZM layout and cross-section are shown in Fig. 1 (a). A series push-pull (SPP) design, where diodes are back-to-back, and G-S electrodes are chosen so that a single RF signal is required to drive the MZM. RF electrodes are defined on both metal layers available in the process to reduce microwave attenuation. A 35- Ω on-chip termination (OCT), intentionally lower than the TW electrode characteristic impedance, is used to peak the device frequency response and extend its bandwidth. The higher doping option is chosen for the pn junctions, improving the V_π at the expense of propagation loss. Since from previous experience the target format for net 200 Gbit/s data transmission is 80 Gbaud PAM-8 [6], the ideal MZM design has 40-50 GHz of bandwidth and maximum phase-shifting efficiency, assuming pulse-shaping with a small roll-off. A phase-shifter length of 2.5 mm is chosen to meet those targets. The MZM phase is tuned with thermal shifters, with a transfer function and IV curve shown in Fig. 1 (b). The measured heater P_π is 18.4 mW. A DC probe is used to bias the central N_{++} doped region and to contact heater pads. Gratings are used to

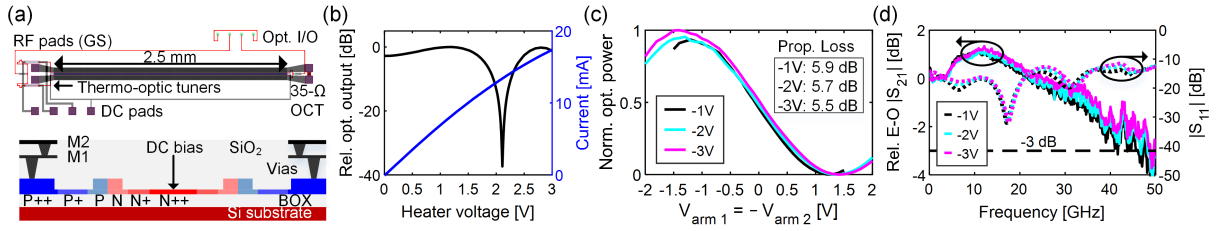


Fig. 1: (a) Top: SPP-MZM schematic. Bottom: phase-shifter cross-section. (b) Thermal tuner transfer function and IV curve. (c) MZM DC transfer function and optical propagation loss vs. reverse bias. (d) MZM small-signal response vs. reverse bias. The $|S_{21}|$ is normalized to 1.5 GHz.

couple light in and out of the chip. Wafer fabrication was carried out in an open-access commercial SOI process. The optical, DC and small-signal characterization of the MZM design is shown in Fig. 1 (c)-(d) for various reverse bias points. In Fig. 1 (c), the DC transfer function (TF) was measured by applying differential voltages simultaneously on the G and S electrodes. This method yields a slightly smaller V_{π} ($V_{TF, top} - V_{TF, bot}$) than typical single-ended methods due to less severe depletion width saturation effects, but is closer to actual operation for SPP MZMs. The extracted DC V_{π} decreases from 5.6 V to 4.8 V as reverse bias approaches 0 V. The device optical loss of 5.7 dB at -2 V bias is largely due to the proximity of the P+ and N+ doped regions with the optical waveguide, which will be corrected in future designs. In Fig. 1 (d), the frequency response was measured with a 50-GHz lightwave component analyzer. RF return loss is <10 dB from 0-50 GHz, and the electro-optic bandwidth is 47 GHz at -2 V, then saturates at deeper bias.

3. Transmission

The experimental setup and DSP are shown in Fig. 2. A single channel from a 120 GSa/s CMOS digital-to-analog converter (DAC) and a 45-GHz RF amplifier constitute the MZM driver. In the transmitter DSP, signal pre-emphasis compensates the driver frequency response up to the 50-GHz RF probe, over a bandwidth set by the raised-cosine (RC) pulse-shaping roll-off. After the chip, we amplify the signal in the optical domain since our 50-GHz O+C band photo-detector (PD) doesn't have a transimpedance amplifier (TIA). The PD optimal received optical power (ROP) is +9 dBm. A 160 GSa/s real-time oscilloscope (RTO) performs analog-to-digital conversion. Fig. 2 also shows the 80 Gbaud PAM-8 electrical signal before the MZM on a digital communication analyzer (DCA), and the spectrum of the corresponding raw received waveform on the RTO. The total signal bandwidth is ~ 88 GHz with a roll-off of 0.1.

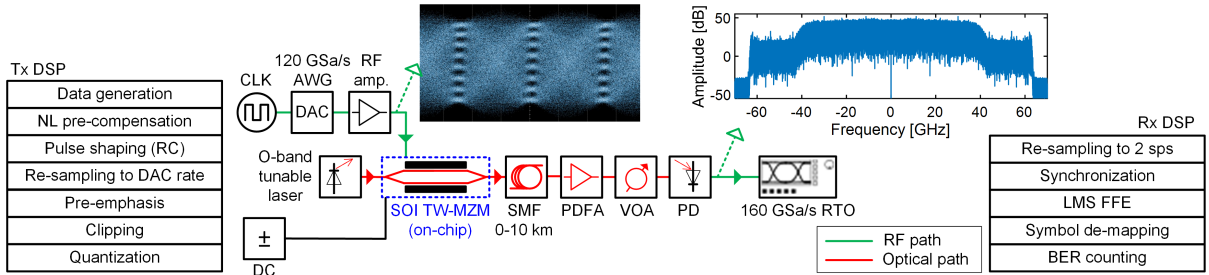


Fig. 2: Experimental transmission setup, transmitter (Tx) and receiver (Rx) DSP, typical 80 Gbaud PAM-8 electrical eye at MZM (RC-shaping at 0.1 roll-off), and corresponding spectrum of raw received waveform at RTO. CLK: clock; AWG: arbitrary waveform generator; PDFFA: Praseodymium-doped fiber amplifier; VOA: variable optical attenuator. LMS-FFE: linear least-mean-square feed-forward equalization (T/2 spaced).

Figure 3 reports transmission results with our SiP MZM design. The empirical optimal bias point is $V_b = -2$ V. Since the maximum driver amplifier output is 2.95 V_{pp} at 80 Gbaud (2.60 V_{pp} at 85 Gbaud), $|V_b| > V_{pp, max}/4$, and continuous reverse bias operation is ensured. In Fig. 3 (a), each data point is the average of 5 RTO captures of 2²⁰ samples. We show successful B2B transmission at 85.5 Gbaud PAM-6 and 2 km transmission at 100 Gbaud PAM-4 under the 3.8E-03 HD-FEC threshold, which respectively represent net rates of 200 Gbit/s and 187 Gbit/s assuming a 6.7% HD-FEC overhead. Note that our PAM-6 data is generated by interleaving in time a 32-QAM complex sequence, for a resulting PAM-6 spectral efficiency of 2.5 bits/symbol [7]. Moreover, from Fig. 3 (a), 80 Gbaud PAM-4 transmission over 10 km under the KP4-FEC threshold is also easily achieved. Selected B2B received eye diagrams after DSP are shown in Fig. 3 (b). We compute in Fig. 3 (c) the normalized generalized mutual information (NGMI) corresponding to the PAM-8 captures of Fig. 3 (a). A reference minimal NGMI threshold of 0.8798 suggests that 2 km transmission at 85 Gbaud PAM-8 (net 212.5 Gbit/s) and 10 km transmission at 80 Gbaud PAM-8 (net 200 Gbit/s) will be error-free after SD-FEC application [8, 9]. Finally, in Fig. 3 (d)-(e), we detail the system sensitivity to MZM drive voltage and to the number of receiver FFE taps, respectively, for 80 Gbaud PAM-8 modulation (net 200 Gbit/s). Only 2.1 V_{pp} is required for B2B transmission at the SD-FEC threshold, or 47 taps at maximum drive voltage.

Finally, we infer from Fig. 3 (a) that, given our system with ~ 45 -50 GHz RF components and the formats tested, the optimal combination to reach net 200 Gbit/s/λ over data-center distances (0-10 km) is 80 Gbaud PAM-8. However, if

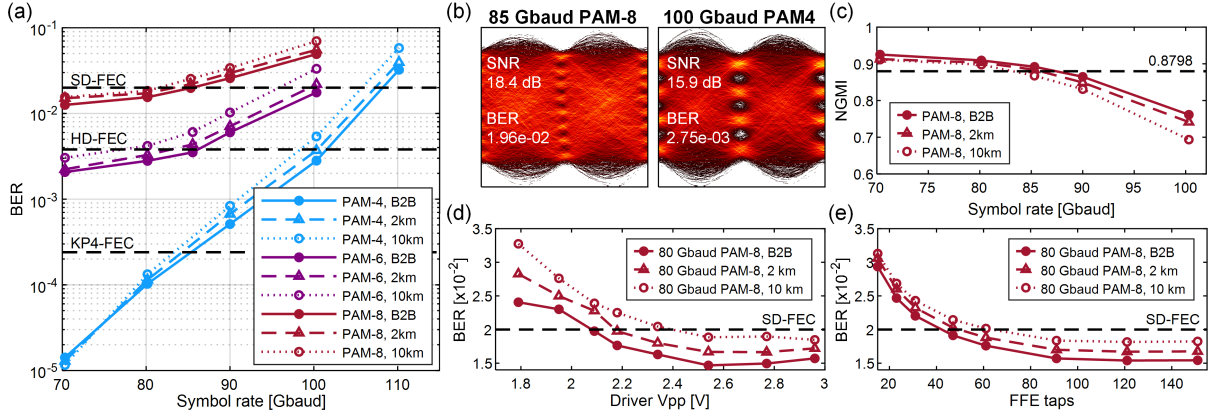


Fig. 3: Data transmission with our SiP MZM. $\lambda_0=1302.8$ nm, $ROP=+9$ dBm. (a) BER vs. symbol rate at B2B, 2 km and 10 km for PAM-4, PAM-6 and PAM-8 formats. (b) B2B received eyes after DSP at 85 Gbaud PAM-8 (net 212.2 Gbit/s) and 100 Gbaud PAM-4 (net 187 Gbit/s). (c) NGMI vs. symbol rate for the PAM-8 data of (a). (d)-(e) BER vs. MZM drive voltage and vs. Rx FFE taps at 80 Gbaud PAM-8 (net 200 Gbit/s). Default drive voltage and taps are 2.95 Vpp and 151, respectively.

very short distances are targeted and using HD-FEC is an important criterion, then 85.5 Gbaud PAM-6 would be the optimal approach. Note that systems with less bandwidth may have different optimal formats for 200 Gbit/s [10].

Table 1 summarizes the -2 V characteristics and 80 Gbaud PAM-8 performance of our MZM design. The MZM energy consumption (E) computation excludes the heater, which consumes $1/2 P_\pi$ in the worst case. Since the pn junction bias consumes negligible power for SPP MZMs, the total MZM power is then ~ 9.2 mW + 12.3 mW = 21.5 mW, or 89.4 fJ/bit, at 80 Gbaud PAM-8 B2B. The maximal transmission distance achievable is limited by ROP.

Table 1: Summary of Modulator Characteristics at -2 V Bias and Performance at 80 Gbaud PAM-8 (Net 200 Gbit/s)

MZM Footprint	Loss	Heater P_π	DC V_π	E-O BW	B2B BER	B2B Min. E (Vpp) ^{a,b}	Max. Dist. ^b
0.9 mm x 3.2 mm	5.7 dB	18.4 mW	5.4 V	47 GHz	1.5E-02	51 fJ/bit (2.1 V)	10 km

^a $E = P_{\text{tot}}/B$ [fJ/bit], $P_{\text{tot}} = V_{\text{RMS}}^2/R$ [mW]. B is the gross bit rate (240 Gbit/s), $R = 35\Omega$ and V_{RMS} is retrieved by integrating the Tx waveform.

^b For BER < 2E-02 SD-FEC threshold.

Compared to our recent results with a segmented SiP MZM [6] and the results of [5] with a dual-drive SiP MZM, the key improvements reported here are the single MZM driver, the absence of complex DSP, the higher net rates and distances achieved, and the transmission of net 200 Gbit/s using the 6.7% HD-FEC threshold. The main enabler of our present results is the superior SiP MZM design in terms of the BW/V_π FOM, which is 8.7 GHz/V at -2 V bias. Our segmented MZM in [6] had a slightly lower bandwidth and significantly higher V_π , and the TW-MZM of [5] has 22.5 GHz bandwidth only (unreported V_π).

4. Conclusion

We presented the design and characterization of an O-band SiP MZM capable of >200 Gbit/s net rate operation. The design has 47 GHz bandwidth, 5.4 V V_π and 5.7 dB loss at -2 V bias. It enables 85 Gbaud PAM-8 transmission over 2 km with 20% SD-FEC (212.5 Gbit/s net rate), with a single 2.6 Vpp driver and linear equalization only. To the best of our knowledge, this is the highest net rate reported for a SiP MZM in a IM/DD system. We also transmit 85.5 Gbaud PAM-6 back-to-back under the 3.8E-03 HD-FEC BER threshold (200 Gbit/s net rate).

5. Acknowledgments

The authors would like to thank Keysight Technologies and Stephane McMeawly for their support.

References

1. M. Bohn *et al.*, "Next-Generation Silicon Photonic Interconnect Solutions", OFC 2019, M3J.3.
2. <https://ethernetalliance.org/technology/2019-roadmap/>.
3. J. Zhou *et al.*, "Silicon Photonics Carrier Depletion Modulators Capable of 85Gbaud 16QAM and 64Gbaud 64QAM", OFC 2019, Tu2H.3.
4. S. Zhalehpour *et al.*, "All-Silicon IQ Modulator for 100 GBaud 32QAM Transmissions", OFC 2019, Th4A.5.
5. Y. Zhu *et al.*, "Towards single lane 200G optical interconnects with silicon photonic modulator", *J. Lightw. Technol.* 38 (1), pp. 67-74, 2019.
6. M. Jacques *et al.*, "200 Gbit/s net rate transmission over 2 km with a silicon photonic segmented MZM", ECOC 2019, PD1.6.
7. J. Wei *et al.*, "225 Gb/s per Lambda IMDD PAM Short Reach Links Using Only Commercial Components", ECOC 2018.
8. D. Che *et al.*, "Single-Channel Direct Detection Reception Beyond 1 Tb/s", OFC 2019, Th4B.7.
9. X. Chen *et al.*, "Generation and intradyne detection of single-wavelength 1.61-Tb/s using an all-electronic digital band interleaved transmitter", OFC 2018, Th4C.1.
10. J. Wei *et al.*, "Experimental comparison of modulation formats for 200 G/λ IMDD data center networks", ECOC 2019.